nature communications

Article

https://doi.org/10.1038/s41467-025-59688-0

Carbamate-bond breaking on bulk oxides realizes highly efficient polyurethane depolymerization

Received: 26 August 2024

Accepted: 30 April 2025

Published online: 09 May 2025

Check for updates

Xinbang Wu[1], Roland C. Turnell-Ritson[1], Peijie Han[2], Jaques-Christopher Schmidt[1], Laura Piveteau[1], Ning Yan[2] ✉ & Paul J. Dyson[1] ✉

Polyurethane is a versatile plastic finding applications across diverse sectors ranging from construction to household products. Recently, there is growing interest in the chemical recycling of polyurethane via catalytic hydrogenation to recover anilines and polyols. However, examples of heterogeneous catalysts are lacking despite their practicality for scale-up to a commercially relevant level. Herein, the conversion of model carbamate compounds is investigated using different metal-oxide catalysts, with CeO_2 exhibiting the best activity and achieving the highest yield of aniline products (up to 100% conversion and 92% yield of anilines). A volcanic correlation is found between the acidity of the metal-oxide catalysts and their activity in cleaving the carbamate bond. The high activity of CeO_2 may be primarily attributed to a low oxygen vacancy formation energy and highly redox active Ce^{3+}/Ce^{4+} pairs. Based on control reactions under different conditions and in situ NMR studies, a mechanism for carbamate bond dissociation on CeO_2 was proposed. Notably, both solvent-free hydrogenation and hydrogen-free transfer hydrogenation approaches may be utilized to depolymerize various commonly encountered polyurethane (thermoplastic and thermoset) products using CeO_2.

The proliferation of plastic waste poses an increasingly pressing environmental challenge for the near future[1]. Developed nearly a century ago by Bayer and co-workers, polyurethanes (PU) represent a type of plastic derived from the addition polymerization of diisocyanates and polyols. PUs are renowned for their versatility and can be modified by selecting different monomer fractions to create a wide array of elastomers, flexible and rigid foams, fibres, adhesives, and coatings[2]. Methylene diphenyl diisocyanate (2,4-MDI or 4,4′-MDI) and toluene diisocyanate (2,4-TDI or 2,6-TDI) are the predominant isocyanate monomers used for PU synthesis[3], due to their lower volatility which allows for safer handling[4]. These monomers are industrially manufactured from the phosgenation of their respective diamines, methylene diphenyl diamine (MDA) and toluene diamine (TDA), which are sourced from commodity feedstocks such as aniline[5]. Therefore, there is an incentive to explore new PU recycling pathways to recover these compounds and reduce the reliance on fossil resources for PU production[6]. Furthermore, the high toxicity of these chemicals poses concern during degradation of PU in the environment, highlighting the importance of implementing appropriate end-of-life treatment[7].

Chemical recycling of PU has been extensively studied, mainly via solvolysis[8,9], aminolysis[10] and glycolysis[11,12] Recently, Gausas et al. reported the depolymerization of PU via a hydrogenation pathway catalysed by a commercially available Ir pincer complex[13]. It was suggested that the catalyst facilitates depolymerization by means of a two-step process, initially breaking the carbamate bond via hydrogenolysis to yield a primary amide and alcohol, followed by hydrogenation of the amide to produce aniline[14]. Metal pincer complexes based on Ru and Mn have also been reported to exhibit activity in PU hydrogenation,

[1]Institute of Chemical Sciences and Engineering, École Polytechnique Fédérale de Lausanne (EPFL), Lausanne, Switzerland. [2]Department of Chemical Engineering, National University of Singapore, Singapore, Singapore. ✉e-mail: ning.yan@nus.edu.sg; paul.dyson@epfl.ch

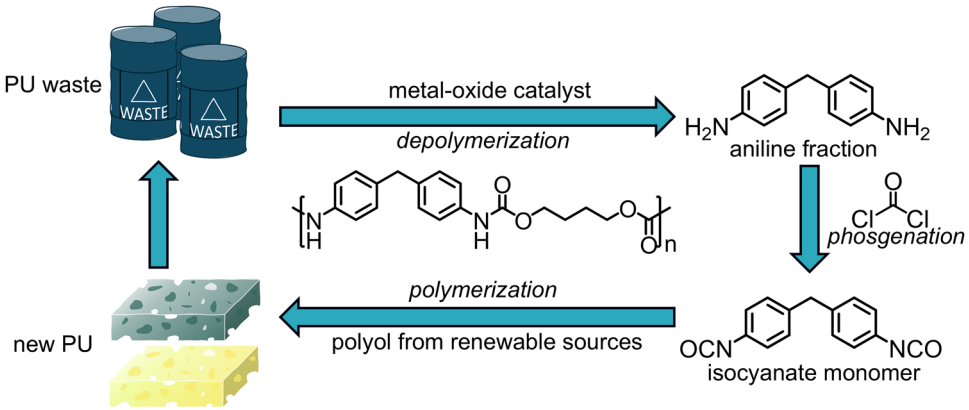

Fig. 1 | Scheme of the proposed circular life cycle of polyurethane (PU). PU waste can be converted using a metal-oxide catalyst into aniline, which is the precursor for synthesizing new polymers.

resulting in high conversion and selectivity towards the aniline products (MDA and TDA)[15,16]. Although isocyanates are the PU monomer, obtaining high yields of their aniline derivatives, which can be readily converted to isocyanates[3], could also be valuable for producing new polymers or other compounds. Nevertheless, the methods employed necessitate the use of a base and homogeneous catalysts, making separation of the catalyst and products challenging, thereby diminishing the overall sustainability of the approach. Ideally, the depolymerization of PU could be conducted in a system that utilizes an inexpensive catalyst that is recoverable and reusable.

Metal-oxide catalysts (MOCs) are the cornerstone of industrial catalysis due to their high abundance and low cost[17], making them promising candidates for PU depolymerization and recycling (Fig. 1). Despite having limited hydrogenation ability compared to noble metal catalysts, MOCs can dissociate hydrogen into surface proton, hydride or hydroxyl species[18,19]. The activity of MOCs depend on various factors, such as surface acid-base sites, electronic structure, and the presence of surface defects[20]. They have been investigated for the depolymerization of polycarbonates into monomers, with the activity of the catalyst found to be correlated to its surface and lattice defects[21]. Herein, various commercially available MOCs, including early transition metals and zeolites, were screened for their activity towards cleaving the carbamate bond in different model compounds, identifying CeO_2 as the most active catalyst. The mechanistic basis for the high activity and selectivity of CeO_2 was elucidated, and the mechanism of carbamate bond dissociation was studied, resulting in the establishment of two different pathways. The first pathway involves using pressurized hydrogen gas under solvent-free conditions, conducted above the melting temperature of PU, to convert thermoplastic PU. The second pathway involves transfer hydrogenation, which uses alcohol as both a solvent and a hydrogen source, to convert both thermoplastic and thermoset PU at lower temperatures.

Results and discussion

Conversion of model carbamate compounds with hydrogenation

The conversion of model carbamate compounds was performed with several commercially available MOCs to assess their ability to cleave the carbamate bond. A simple analogue of PU, phenylurethane (M1), and dicarbamates containing the MDI monomer—ethane-1,2-diylbis((4-benzylphenyl)carbamate) (M2) with aromatic terminal groups and dibutyl(methylenebis(4,1-phenylene))dicarbamate (M3) with butyl terminal groups—were selected as the model compounds for screening (Fig. 2). The catalysts were annealed at 550 °C in air before reaction in order to activate them (see Supplementary Fig 1 for powder X-ray diffraction patterns). The reactions were performed without a solvent under 10 bar H_2 at 200 °C, the temperature at which hydrogen dissociates on the catalyst surface[22].

It should be noted that all model compounds underwent some conversion in the control reaction without any catalyst, reflecting the low thermal stability of the carbamate species[23]. However, adding a catalyst improved both the overall conversion and yield of the aniline and alcohol products, but to varying extends. Among the MOCs, CeO_2 achieved near-quantitative conversions of the model compounds with an outstanding yield of aniline products, i.e. 100% conversion of M1 with 92% aniline, 100% conversion of M2 with 90% 4-benzylaniline (4-BA), and 94% conversion of M3 with 92% 4,4′-MDA. In contrast, the selectivity of CeO_2 to forming alcohol products was considerably lower, at 22% ethylene glycol selectivity and 67% 1-butanol selectivity from the conversion M2 and M3, respectively. The yield of ethanol (EtOH) from M1 was not quantified as it overlaps with the solvent peak in the GC-MS spectrum (Supplementary Fig 2). The lower alcohol selectivity was attributed to the mechanism of carbamate bond cleavage on CeO_2 (see below).

Besides aniline, phenylisocyanate was also detected from the conversion of M1, but only for reactions with low overall conversion (Supplementary Table 1). MOCs that achieve high conversion, including CeO_2, acidic γ-Al_2O_3, $AlCeO_3$ and La_2O_3, do not afford phenylisocyanate under these conditions. Other aromatic species detected in trace amounts include dimers and trimers of imine and urea, presumably produced from side reactions involving aniline or phenylisocyanate. A prolonged reaction time can lead to these undesired side reactions[24,25], hence control of reaction time is an important factor for achieving high selectivity to anilines. The conversion of M1 with CeO_2 was performed over different durations (Supplementary Table 4), with the yield of aniline decreasing as the reaction extends beyond 2 hours. Phenylisocyanate was detected after 1 hour of reaction, suggesting that it is formed before aniline. It is likely that an equilibrium exists between the carbamate and the products, as CeO_2 has been reported to be active for the formation of carbamate or urea[26]. Interestingly, no traces of aryl or cyclohexyl species, such as benzene or cyclohexylamine, were observed even after 5 hours of reaction, indicating the absence of aniline C–N bond cleavage or ring-hydrogenation. This observation reveals the poor capacity of MOCs for hydrogenation, making them suitable catalysts for the selective cleavage of the carbamate bond.

For the conversion of M2 and M3, the catalysts generally achieved a higher aniline product yield for M2 and a higher alcohol yield for M3, due to only one carbamate bond being cleaved. Higher conversion was achieved for M2 compared to M3 due to an extended reaction time of 3.5 hours. Similar to M1, prolonging the reaction time for the CeO_2-catalysed reactions leads to a decrease in yield of both the aniline and

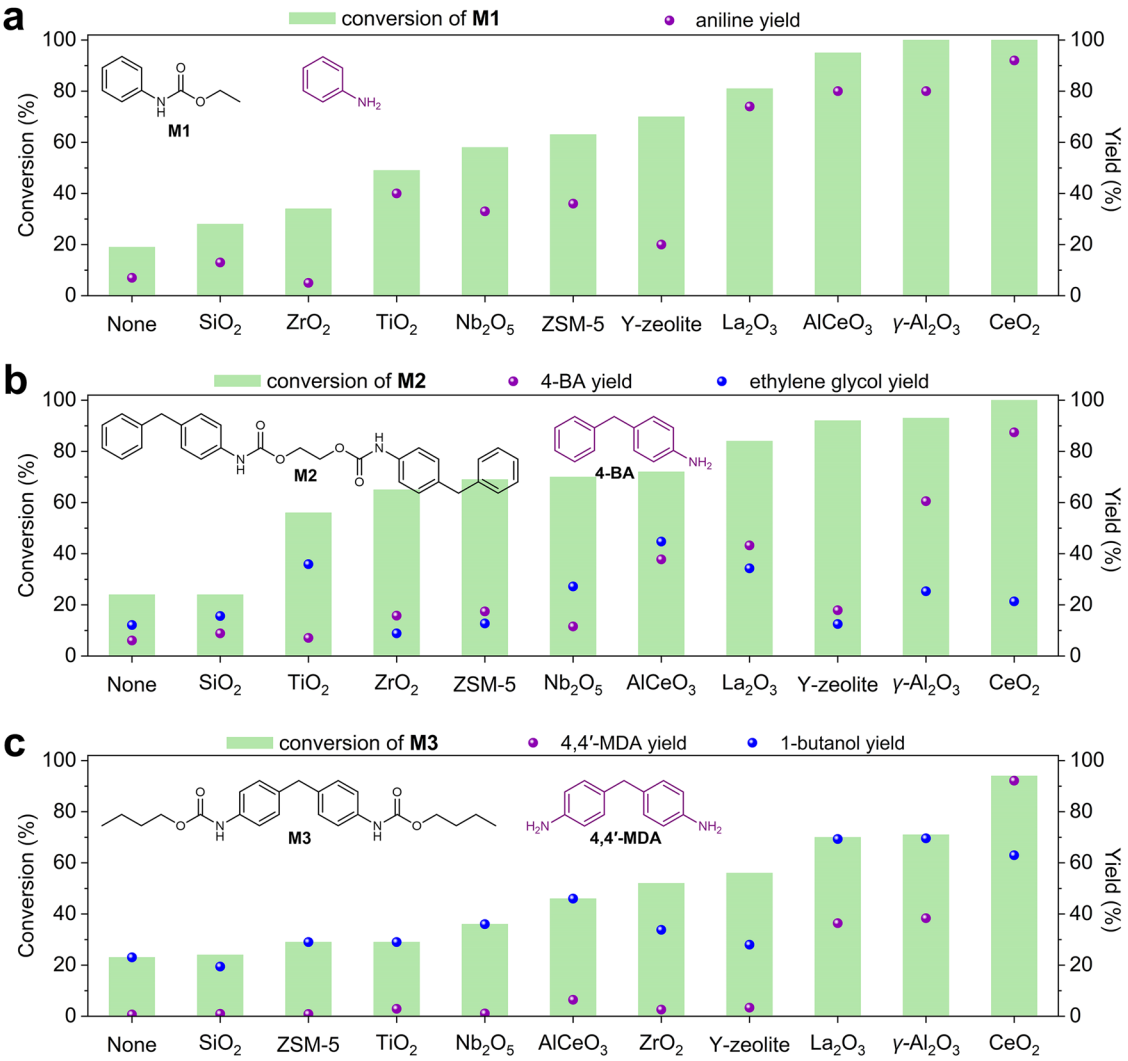

Fig. 2 | Catalyst screening for the conversion of model carbamate compounds using various MOCs. Yield of aniline and alcohol (only for M2 and M3) products from the conversion of (**a**) M1, (**b**) M2 and (**c**) M3, yield of ethanol from the conversion of M1 was not quantified. Reaction conditions: model carbamate (250 mg), catalyst (25 mg), H_2 (10 bar), 200 °C, 2 hours (M1 and M3) and 3.5 hours (M2). The products were analysed using GC-MS. Full data of the conversions is available in Supplementary Tables 1-3.

alcohol products (Supplementary Tables 5 and 6). In addition to the reduction in aniline product yield due to dimerization, the yield of alcohol products also decreases due to dehydrogenation occurring on CeO_2[27,28]. A fraction of the alcohol products likely remains adsorbed on the catalyst after the reaction, as evidenced from thermal gravimetric analysis (TGA) of the spent CeO_2 following the conversion of M2 (Supplementary Fig 3). Furthermore, the direct correlation between the CO_2 yield and the overall conversion (Supplementary Tables 1-6) suggests that a portion of the alcohol products was converted to CO_2[29], which was the only gaseous product detected. The surface oxygens of CeO_2 are suspected to be involved in the formation of CO_2, where oxygen from the bulk can replace depleted surface oxygens via a Mars-van Krevelen mechanism[30,31].

From the catalyst screening, CeO_2 emerged as the most promising MOC for investigating PU depolymerization. The CeO_2 catalyst exists as nanoparticles of diameter <30 nm (Supplementary Fig 5), with a high BET surface area of 42 m^2/g (Supplementary Table 8), and has an excellent tolerance for polar molecules, such as water, which tend to inhibit the active sites of other MOCs[32,33]. ICP-MS analysis revealed negligible metal impurities in the catalyst (Supplementary Table 9), indicating that the high activity was attributed to CeO_2. As Lewis acids have been previously reported to catalyse the conversion of PU to isocyanates[34], the Lewis acidic sites of the MOCs were suspected to be the active sites for carbamate bond cleavage. Temperature-programmed desorption of ammonia (NH_3-TPD) measurements were performed to compare the acidity of the MOCs (Fig. 3a), where the integral at the first desorption maxima in the spectra was used as a relative comparison of total surface acidity (Supplementary Fig 4). Interestingly, the correlation observed between carbamate bond cleaving activity and catalyst acidity follows a volcanic distribution (Fig. 3b), with CeO_2 exhibiting higher catalytic activity despite having a lower overall acidity than ZSM-5, zeolite-Y and acidic γ-Al_2O_3, which are all irreducible MOCs. ^{31}P solid-state NMR spectroscopy was performed using tributylphosphine oxide (TBPO) to probe the Lewis and Brønsted acid sites in CeO_2 and γ-Al_2O_3 (Supplementary Fig 6), revealing that CeO_2 contains a significantly lower Lewis acidic site density than γ-Al_2O_3 (0.076 vs. 1.074 mmol/g). This suggests that in addition to Lewis acidity, other factors play a key role in carbamate conversion. Potential factors include catalyst reducibility and amount of surface oxygen vacancies, where CeO_2 has a lower surface oxygen vacancy formation energy compared to the other MOCs[35]. To confirm this hypothesis, CeO_2 was annealed under argon at different temperatures to investigate the effect of oxygen vacancies on the conversion of the model compounds (Fig. 3c). More oxygen vacancies are generated when the

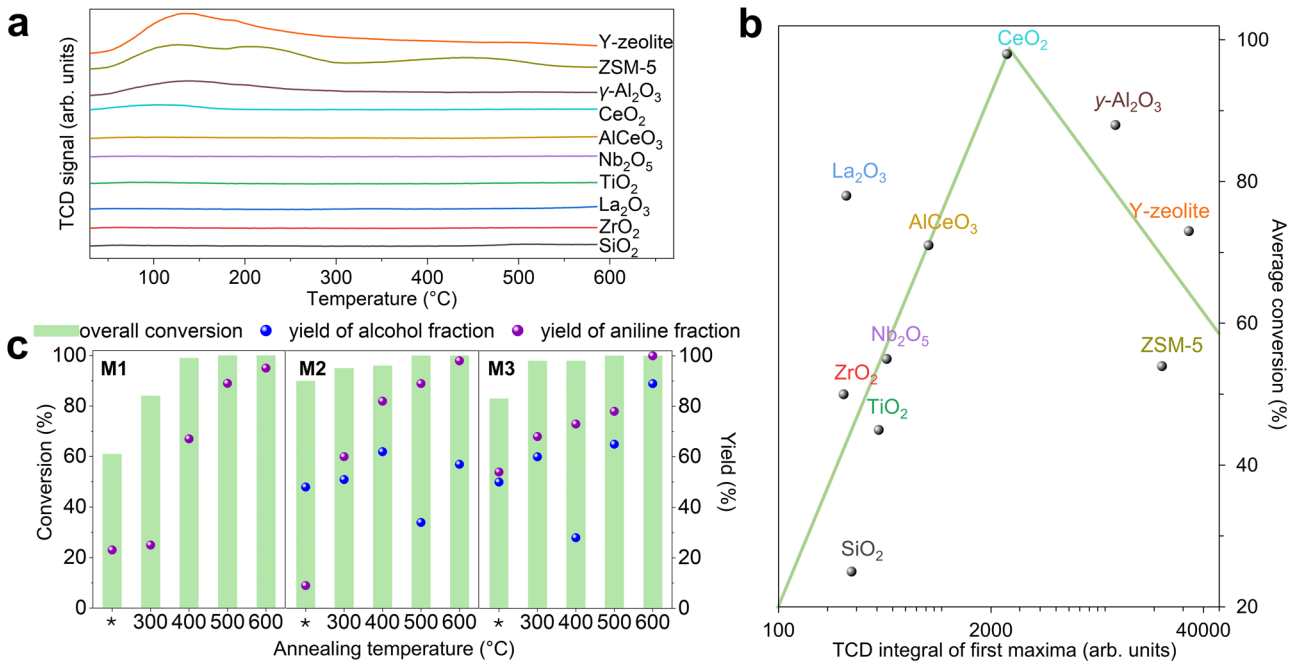

Fig. 3 | Investigation of catalyst properties governing carbamate bond cleaving activity. a NH_3-TPD spectra of the MOCs. The temperatures for the first ammonia desorption maxima are shown in Supplementary Fig 4. **b** Volcano correlation between total acidity and carbamate bond cleaving activity of the MOCs. The y-axis represents the average conversion of the model compounds achieved by each catalyst. **c** Conversion of the model compounds using CeO_2 annealed under argon at different temperatures. * Unannealed CeO_2. Reaction conditions: model carbamate (250 mg), catalyst (25 mg), H_2 (10 bar), 200 °C, 2 hours (M1 and M3) and 3.5 hours (M2). Full data of the conversions is available in Supplementary Table 7.

oxide is annealed at higher temperatures[24], and CeO_2 achieves full conversion of the model carbamates after annealing at temperatures above 500 °C. Notably, both the conversion and selectivity to aniline products increase with higher annealing temperatures, suggesting that surface oxygen vacancies play a role in the formation of aniline. Furthermore, the high reducibility of Ce^{4+} to Ce^{3+} in CeO_2 may explain its superior activity compared to $AlCeO_3$[36]. Although CeO_2 annealed using the typical procedure (at 550 °C under air) showed slightly lower activity than the CeO_2 annealed at 600 °C under argon (98% average conversion vs. 100% average conversion), it was used for further studies due to its lower cost of preparation and regeneration.

To investigate the effect of hydrogen during carbamate bond cleavage, M2 was reacted under 1 bar H_2 in the presence of CeO_2, resulting in 83% conversion (Supplementary Table 10, entry 6). Increasing the pressure to 50 bar H_2 did not result in significant improvement in the rate of reaction (Supplementary Table 10, entry 5), which suggests that the conversion is not fully dependant on hydrogen pressure. Surprisingly, conversion also occurred under the inert and oxidising atmospheres of nitrogen and air, albeit with lower alcohol and aniline product yields. The hydrogen required to generate the aniline products under these conditions may originate from the dehydrogenation or dehydration of the alcohol on CeO_2[37], e.g. ethylene glycol may be converted to either hydrogen and ethylenedioxyl, or water and CO_2 during the conversion of M2[38]. Furthermore, the ^1H NMR spectrum of the product mixture after the conversion of M1 under 10 bar D_2 reveals a higher-than-expected proton count for EtOH (-OH) and aniline (-NH_2/-NHD) (Supplementary Fig 7), suggesting that hydrogen from the carbon chain in EtOH may be partially consumed for hydrogenation of the carbamate bond. To examine whether water plays a role during the conversion, it was introduced to the reaction conducted under nitrogen (Supplementary Table 11). The high conversions of 100%, 94% and 97%, for M1, M2 and M3, respectively, indicate that the reactions are enhanced by the presence of water. This is presumably due to the formation of more hydroxyl species on the CeO_2 surface[39], which could be generated from either the deprotonation of water or the dissociation of hydrogen[40,41]. Notably, the conversion of the model compounds decreases significantly when water is used as a solvent, possibly due to the poor solubility of the aromatic carbamates.

Transfer hydrogenation of model compounds with CeO_2

Instead of water, alcohols can be used as a source of protons for transfer hydrogenation reactions, especially in the presence of an excellent dehydrogenation catalyst such as CeO_2[42], producing active surface hydroxyls[27]. In addition, alcohols disperse PU and its monomers, which could facilitate improved surface contact between the catalyst and the reactant. This is particularly useful for converting thermoset PU, which does not soften at high temperatures[3]. The feasibility of the transfer hydrogenation pathway for PU depolymerization was investigated using the model compounds in alcohol solvents (Fig. 4). The reactions were first performed using isopropanol (*i*PrOH) as the solvent, at 160 °C for 24 hours. Under these conditions, CeO_2 achieved near quantitative conversion of all model compounds. In comparison to the hydrogenation pathway, the yield of aniline products decreases due to side reactions resulting from the extended reaction time. In addition, the alcohol solvent is able to react with the aniline products to form secondary and tertiary imines or amines[24].

Since EtOH is cheaper than iPrOH, and bio-EtOH can be readily derived at scale from renewable sources[43], it was compared as the hydrogen source. Gratifyingly, high conversions of M2 (98%) and M3 (74%) were also achieved after 24 hours when using EtOH as the hydrogen donor, due to the strong dehydrogenating ability of CeO_2, allowing further exploration of EtOH as a solvent for PU depolymerization. Reducing the reaction time to 2 hours resulted in only 15% conversion of M2 in EtOH (Supplementary Table 12, entry 6). The conversion increases to 41% when 10 bar H_2 was added (Supplementary Table 12, entry 7), presumably due to the additional hydrogen reducing CeO_2 to generate more surface hydroxyl species or oxygen vacancies that promote transfer hydrogenation[44]. At 200 °C, 99% conversion of M2 was achieved after 3.5 hours in EtOH under air

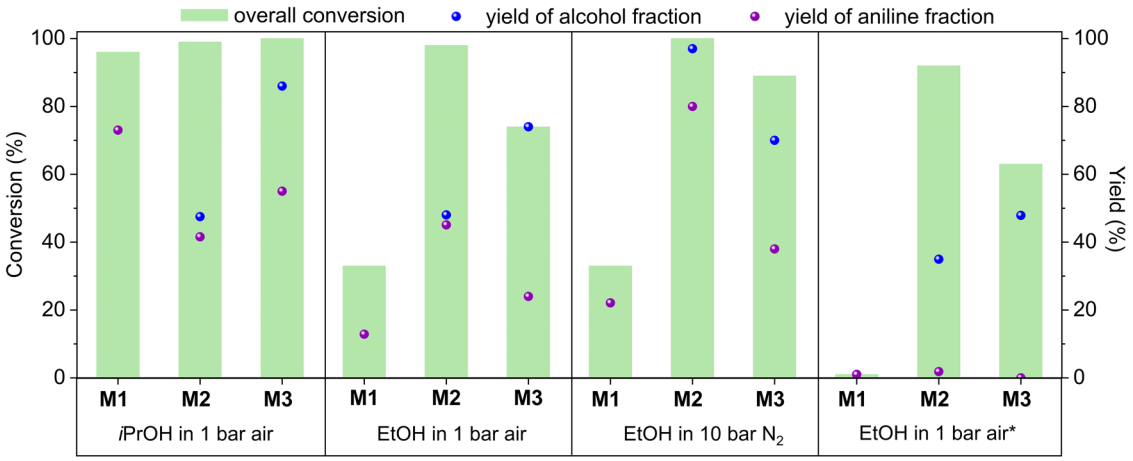

Fig. 4 | Conversion of the model compounds catalysed by transfer hydrogenation using CeO_2 as the catalyst and alcohols as the hydrogen donor. Reaction conditions: model carbamate (250 mg), CeO_2 (25 mg), solvent (2 mL), 160 °C, 24 hours. *Without catalyst. Full data of the conversions is available in Supplementary Table 12.

(Supplementary Table 12, entry 8), although the yield of 4-BA was lower compared to the solvent-free reaction performed under H_2 (58% vs. 90%), due to further reactions with the solvent. The high conversions achieved in both pathways signifies that CeO_2 exhibits similar reactivity under both conditions, and the temperature for the transfer hydrogenation pathway must be controlled to avoid side reactions.

Compared to M2 and M3, the conversion of M1 in EtOH at 160 °C was distinctly lower, at only 33% after 24 hours, presumably as EtOH is also the alcohol product from the reaction. When the conversion of M1 was performed in methanol, phenylisocyanate and methylbenzylcarbamate were detected (Supplementary Fig. 8). Methylbenzylcarbamate could be generated from the reaction of phenylisocyanate with methanol, suggesting that the isocyanate is an intermediate species during transfer hydrogenation, which explains the significantly lower conversion of M1 in EtOH, as the reverse reaction could readily occur. Overall, an improvement in alcohol yield was obtained from the transfer hydrogenation pathway compared to the hydrogenation pathway. This was particularly evident in the conversion of M2, with the yield of ethylene glycol increasing from 22% (under the hydrogenation pathway) to 48% when the reaction was performed in EtOH. The improved yield likely results from the lower reaction temperature used, which disfavours side reactions of the alcohol products[37,45]. These reactions can be further mitigated by using an inert N_2 atmosphere, leading to an increased improvement in the ethylene glycol yield, to 76% (Supplementary Table 12, entry 12). The reactions performed in EtOH without CeO_2 catalyst reveal that the bicarbamates M2 and M3 are highly susceptible to nucleophilic addition by the EtOH solvent. Although high conversions of M2 and M3 were achieved without catalyst, there was negligible aniline products yielded. Thus, the CeO_2 catalyst modulates formation of anilines, presumably by strong binding of highly reactive isocyanate intermediates to prevent the reformation of carbamates.

The conversion of M1 was also performed in deuterated ethanol (d_6-ethanol) at 120 °C and the reaction was monitored in situ by NMR spectroscopy. From analysis of the ^{13}C NMR spectra, the only products detected during the reaction were aniline and EtOH (Fig. 5a). Under these conditions, peaks for phenylisocyanate were not observed. In contrast, peaks corresponding to phenylisocyanate were observed in the ^{13}C NMR spectra acquired after the reaction mixture was cooled to room temperature (Supplementary Fig 9). This suggests that phenylisocyanate is adsorbed on the CeO_2 surface during the reaction, with its transformation to aniline rapidly occurring at 120 °C. The detection of isocyanate in both the hydrogenation and transfer hydrogenation reactions suggests that the two pathways follow the same tentative mechanism proposed in Fig. 5b. First, hydrogen dissociation or alcohol deprotonation at the Lewis acid sites will generate hydroxyl species and oxygen vacancies on the CeO_2 surface[39], where the carbamate will be adsorbed, weakening (activating) the C-OR bond. After adsorption, the carbamate bond dissociates, generating an alcohol and an intermediate isocyanate species, similar to previous studies involving Lewis acids[34]. The isocyanate can readily react with a surface hydroxyl species to form carbamic acid, which spontaneously decomposes to CO_2 and the aniline product. It is possible that the lower energy required to generate oxygen vacancies on CeO_2, compared to other MOCs[35], allows rapid release of a surface hydroxyl to stabilize the isocyanate intermediate after carbamate dissociation, rationalizing its high activity. Furthermore, as long as the alcohol remains adsorbed on CeO_2, the reverse reaction will not occur, thereby driving the formation of aniline. Besides recombination with the isocyanate intermediate, the adsorbed alcohol could also either undergo dehydrogenation or be protonated and released. The strong dehydrogenation ability of CeO_2 improves the aniline product yield at the expense of the alcohol.

This mechanism differs from the two-step mechanism previously proposed for metal-catalysed carbamate bond cleavage, which first generates an amide that is then further hydrogenated to the aniline product[14]. Interestingly, carbamate dissociation on MOCs produces isocyanate, which is the direct monomer for PU, as an intermediate species. However, the removal of free alcohol from the reaction system is necessary to prevent recombination with isocyanate. The isocyanate is also highly reactive towards water and surface hydroxyl species, making it challenging to isolate.

Conversion of PUs

The conversion of a model PU, PU-1 (synthesized using 4,4'-MDI and 1,6-hexanediol (M_w ~1300 g/mol, see Supplementary Fig 10 for the ^1H NMR spectrum), was studied in detail (Fig. 6a). PU-1 undergoes full depolymerization at 200 °C after 4 hours, affording 4,4'MDA and 1,6-hexanediol in 97% and 89% yields, respectively. Interestingly, the 1,6-hexanediol yield obtained from the depolymerization reaction is higher than the yield of ethylene glycol from the conversion of M2, presumably due to the lower reactivity by virtue of the longer carbon chain (C_6 vs C_2). Increasing the reaction time gives a trend similar to that seen for the model compounds, with the yield of aniline and alcohol products decreasing as they react further to afford byproducts (Supplementary Table 13). For instance, 4-cyclohexanediol and oxepines were observed from the dehydrogenation or dehydration of 1,6-hexanediol after 8 hours. When

https://doi.org/10.1038/s41467-025-59688-0

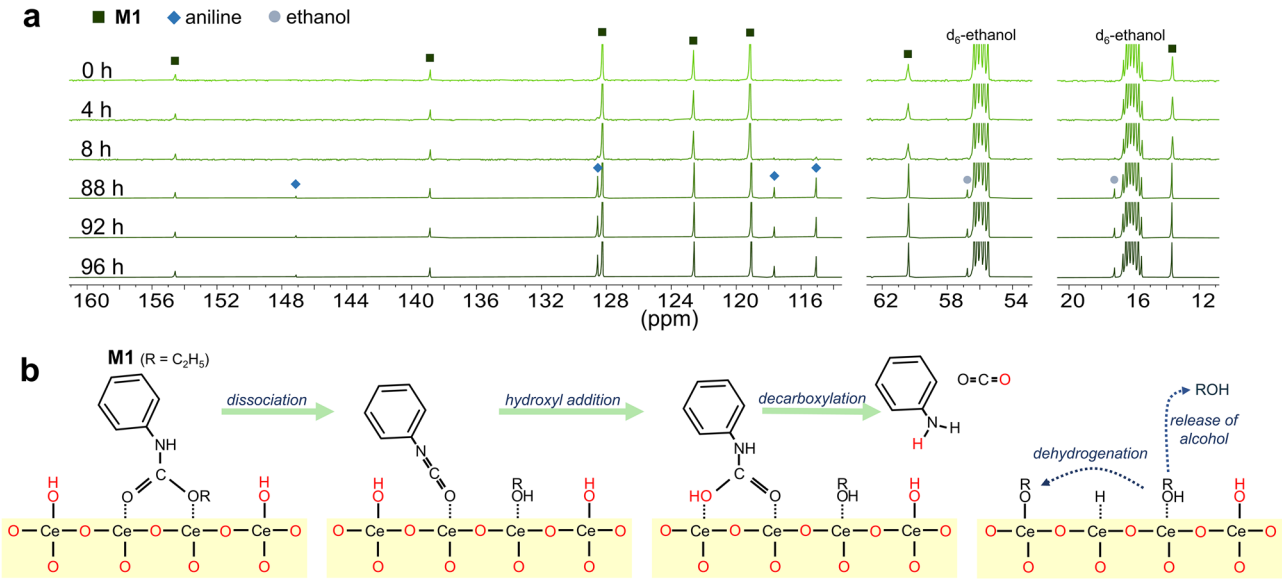

Fig. 5 | Probing the mechanism of carbamate bond activation and cleavage. a In-situ ^{13}C NMR spectra for the conversion of M1 in d_6-ethanol at 120 °C. Reaction conditions: M1 (50 mg), CeO_2 (50 mg), d_6-ethanol (2 mL), 120 °C, 96 hours. **b** Proposed reaction mechanism showing the conversion of M1 on a hydroxylated CeO_2 surface.

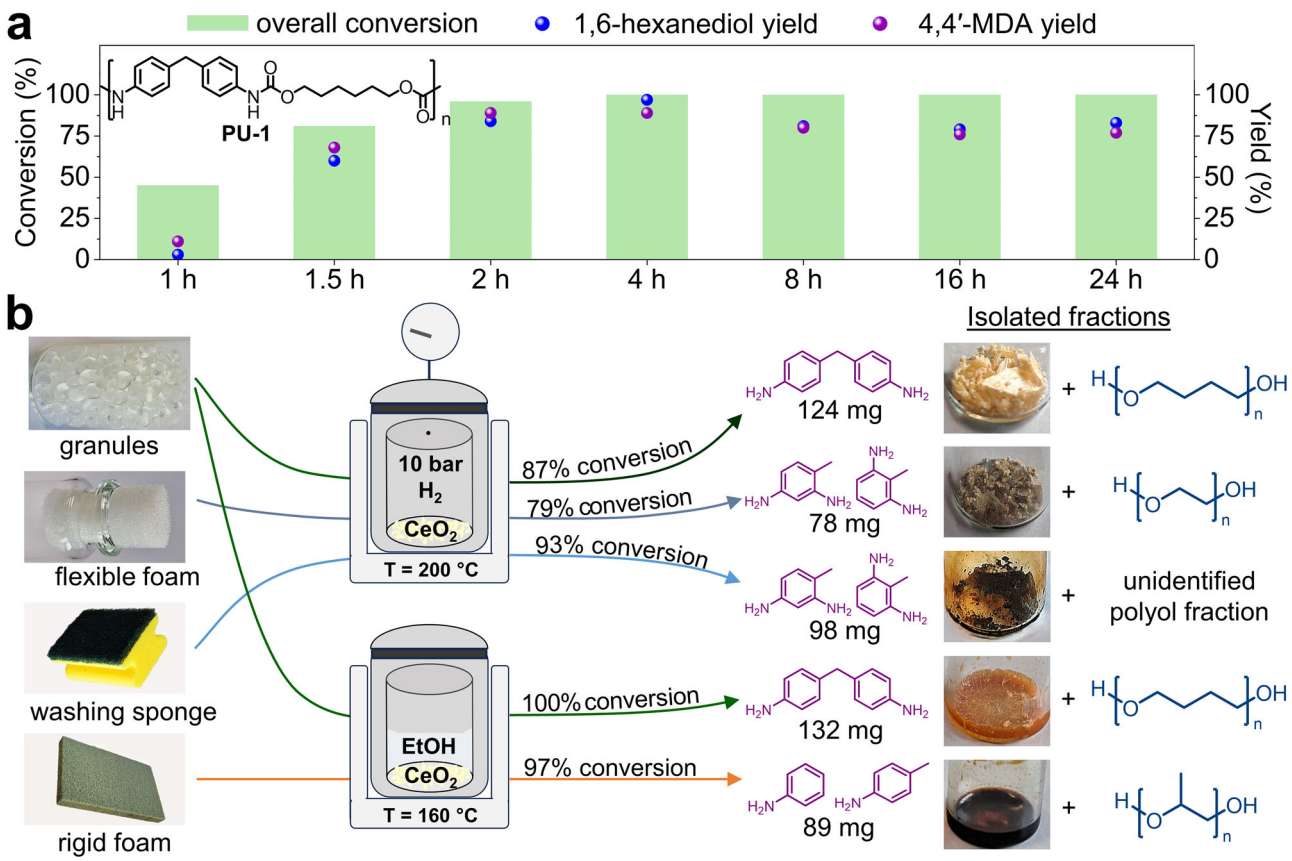

Fig. 6 | Conversion of PUs. a Conversion of model PU-1 using CeO_2 via the hydrogenation pathway, with separate reactions performed for different durations. Reaction conditions: PU-1 (250 mg), CeO_2 (25 mg), H_2 (10 bar), 200 °C. **b** Conversion of commercial PU products using CeO_2 via both hydrogenation and transfer hydrogenation pathways. Reaction conditions: PU (500 mg), CeO_2 (50 mg), H_2 (10 bar), 200 °C, 8 hours for the hydrogenation pathway, and EtOH (5 mL), 160 °C (thermoplastic PU), 180 °C (rigid PU foam), 14 hours for the transfer hydrogenation pathway. Full data of the reactions of (**a**) and (**b**) are available in Supplementary Tables 13 and 15, respectively.

compared to CeO_2, acidic γ-Al_2O_3 resulted in a lower PU-1 conversion of 79%, with 45% 4,4′-MDA yield after 24 hours (Supplementary Table 13, entry 10). Apart from trace amounts of *N*-methylated side products (~3%)[46], such as 4,4′-methylenebis(N,N-dimethylaniline), the remainder of the aniline fraction likely remained as diethyl ether-soluble oligomers due to the lower catalytic activity of γ-Al_2O_3.

Subsequently, the conversion of thermoplastic PU granules (M_w ~120,000 g/mol, NMR spectra shown in Supplementary Fig. 11) was tested using CeO_2. Due to its high elasticity and high tensile strength,

thermoplastic PU is becoming increasingly prominent in various manufacturing applications, including 3-D printing[47,48]. It is well-suited for depolymerization via the hydrogenation pathway as its melting point is below 200 °C, and the M_w of the THF-soluble residue decreased to 40,600 g/mol after 1 hour (12% conversion, Supplementary Table 14). The conversion rate of thermoplastic PU granules is slower than that of PU-1, presumably due to its higher M_w and the presence of additives, such as crosslinkers and plasticizers, used in commercial PU. The solid residue collected after 3 hours (71% conversion) has a M_w of ~3000 g/mol, with only a slight decrease in the M_w observed for residues from reactions performed at longer durations. After 8 hours of reaction, 87% of the thermoplastic PU granules was converted into diethyl ether-soluble compounds, compared to less than 1% conversion in the control reaction (without catalyst, Supplementary Table 15, entry 2), and 4,4′-MDA was obtained as the only aniline product (Supplementary Fig 12). 124 mg of 4,4′-MDA was isolated from the product mixture using flash-column chromatography, corresponding to 81% yield based on the aniline-to-polyol ratio obtained from ^{1}H NMR spectroscopy of the polymer. Additionally, a butanediol-based polyol fraction was also isolated from the reaction. This promising result demonstrates the solvent-free depolymerization of a commercial PU into its aniline derivatives (Fig. 6b). To evaluate the reusability of the catalyst, the spent CeO_2 was reused directly in a subsequent reaction after drying at 80 °C for 16 hours, without any additional treatment. The catalyst achieved 64% conversion after 24 hours reaction time due to partial deactivation. However, the CeO_2 catalyst could be regenerated by calcination in air at 550 °C (see Supplementary Methods for regeneration procedures), upon which its activity was restored in full. This process was repeated for five reaction cycles with negligible change in catalytic activity (Supplementary Fig 13). The transformation of thermoplastic PU granules was also investigated via the transfer hydrogenation pathway in EtOH. After 14 hours of reaction at 160 °C, full conversion of the polymer was achieved (Supplementary Fig 14). The isolated yield of 4,4′-MDA of 132 mg (86%) closely resembled the yield obtained from the hydrogenation reaction (81%), demonstrating the feasibility of both pathways.

The substrate scope was then extended to other commercial PU products, including a flexible foam used as a stopper, a rigid foam used for insulation (Tricast-5), and a common washing sponge. The flexible foam (M_w ~13,000 g/mol), which is a thermoplastic, is capable of undergoing depolymerization via solvent-free hydrogenation. A conversion of 79% was obtained after 8 hours and the isolated aniline fraction (78 mg) was found to contain a mixture of 2,4-TDA and 2,6-TDA with a 3:1 ratio (Supplementary Fig 15). The polyol fraction was identified as polyethylene glycol and accounted for the majority of the mass yield (302 mg), primarily contributing to the flexibility of the foam. Next, the PU component of a washing sponge was separated from its scouring pad and investigated for conversion via hydrogenation. Although the sponge is also a flexible PU foam, it contains additives, such as surfactants, colorants and softening agents[49,50], which have the potential to hinder the reaction or poison the catalyst[51]. Remarkably, a conversion of 93% was achieved after 8 hours, surpassing even the conversion rate of the pure thermoplastic PU granules, likely due to the lower molecular weight of the sponge (M_w ~8000 g/mol). The isolated aniline fraction (98 mg) was found to contain both 2,4-TDA and 2,6-TDA in a 2:1 ratio (Supplementary Fig. 16). The presence of additives did not decrease the activity of the catalyst nor the selectivity to aniline, highlighting the resilience of CeO_2 to poisoning compared to noble metal catalysts. To explore the scalability of the process, the conversion of the sponge was repeated on a larger scale, using an entire sponge, including the scouring pad (Supplementary Fig. 17). Remarkably, 91% conversion was achieved and 1.02 g of TDA was isolated (21 wt.% of initial sponge) using the hydrogenation pathway, demonstrating the potential for scaling-up the reaction to convert actual thermoplastic PU waste.

Lastly, the conversion of the high-density rigid PU foam was explored. As the foam is a thermoset, it does not soften at elevated temperatures, which poses a challenge for conversion via the hydrogenation pathway. Consequently, only 8% conversion was achieved under solvent-free conditions, although visible changes to the foam was observed after reaction (Supplementary Fig. 18). The transfer hydrogenation pathway was employed to improve the conversion, with the reaction conducted in EtOH at 160 °C. After 14 hours, a conversion of 55% was obtained, with the major products being aniline and *p*-toluidine. These products are presumably obtained from the deamination of TDA over a prolonged reaction time[52]. Due to the high durability of the rigid foam[13], near-complete conversion was only achieved by increasing the reaction temperature to 180 °C. Despite the high conversion, only monoaniline products (89 mg) were isolated from the depolymerization of the rigid PU foam (Supplementary Fig. 19). These examples demonstrate the effective conversion of commonly encountered PU-based products using CeO_2 as a heterogeneous catalyst.

In summary, we identified CeO_2 as an outstanding heterogeneous catalyst for the depolymerization of PUs. Among several MOCs tested, CeO_2 achieved the highest overall conversion and selectivity to anilines. Isocyanate was identified as a key intermediate species during carbamate bond dissociation. The highly redox active Ce^{3+}/Ce^{4+} pairs in CeO_2 allow it to act as an oxygen source for the conversion of the isocyanate into CO_2 and aniline. Two pathways for PU depolymerization were demonstrated. The hydrogenation pathway aligns with current hydrogenolysis methods for plastic recycling and can be performed under solvent-free conditions[53], whereas the transfer hydrogenation pathway is capable of converting thermoset PU by employing a renewable solvent, such as EtOH, and can achieve a higher yield of the polyol fraction. As CeO_2 is relatively inexpensive compared to noble metals and is widely utilized in catalytic converters[54], there is considerable potential to adopt CeO_2 as a catalyst for PU recycling.

Methods

Materials

Cerium(IV) oxide, aluminium cerium(III) oxide, niobium(V) pentoxide, acidic gamma-alumina oxide, methylenediphenyl-4,4′-diisocyanate, 1-butanol, 1,6-hexanediol, 4-benzylaniline, ethylenebis(chloroformate) and dibutyltindilaurate were purchased from Sigma-Aldrich. Phenylurethane (M1) was purchased from TCI. Zirconium(IV) oxide, silicon dioxide, Y-zeolite and ZSM-5 zeolite were purchased from acbr GmbH. Titanium(IV) oxide was purchased from Fluka. TBPO was purchased from Chemie Brunschwig. Lanthanum(III) oxide was purchased from Strem Chemicals. Thermoplastic PU granules and rigid PU foam (Tricast-5) were purchased from Goodfellow. Flexible PU foam stoppers were purchased from Thermo Fisher.

Reaction procedure: hydrogenation method

In a typical hydrogenation reaction, 25 mg (50 mg) of catalyst and 250 mg of model compound (500 mg of PU) was added to a pre-weighed glass vial with a stir-bar. The vial was transferred into a stainless-steel Parr autoclave (volume 75 mL) and was tightly sealed. The autoclave was pressurized to 10 bar of H_2 and underwent five purge cycles. The autoclave was placed in a pre-heated Parr ceramic heater at 200 °C with stirring maintained at 700 r.p.m. At the end of the reaction, the autoclave was placed under running water in a water-bath until cooled.

Reaction procedure: transfer-hydrogenation method

In a typical transfer-hydrogenation reaction, 25 mg (50 mg) of catalyst, 250 mg of model compound (500 mg of PU) and 2 mL (5 mL) of ethanol was added to a pre-weighed glass vial with a stir-bar. The vial

was transferred into a stainless-steel Parr autoclave (volume 75 mL) and was tightly sealed. The autoclave was placed in a pre-heated Parr ceramic heater at 160 °C with stirring maintained at 700 r.p.m. At the end of the reaction, the autoclave was placed under running water in a water-bath until cooled.

Product analysis: model compounds

The autoclave was depressurized and the gaseous products were collected in a balloon for GC-FID analysis. The yield of CO_2 was quantified using a calibration curve and calculated as the percentage carbon balance of the reactant. The glass-vial was removed from the autoclave and the products were extracted with diethyl ether (M1) or methanol (M2, M3 and PU-1). The insoluble fraction, containing catalyst and reactant, was separated from the soluble fraction via centrifugation. The insoluble fraction was dried for 1 hour at 80 °C and weighed for the conversion calculation for M2, M3 and PU-1 using Eq. (1).

$$\text{Conversion} = \left(1 - \frac{\text{Mass of insoluble fraction} - \text{Mass of catalyst}}{\text{Mass of initial reactant}}\right) \times 100\% \quad (1)$$

The conversion of M1 was determined from GC-MS analysis using a calibration curve. The liquid fraction was analysed using GC-MS with hexadecane (M1) or *p*-xylene (M2, M3 and PU-1) as an internal standard. The yields of the aniline and alcohol fractions were calculated using Eq. (2).

$$\text{Yield of aniline or alcohol} = \frac{\text{Mol of aniline or alcohol quantified from GC} - \text{MS}}{\text{Mol of aniline or alcohol present in the reactant}} \times 100\% \quad (2)$$

Product analysis: commercial PU

The glass-vial was removed from the autoclave and the products were extracted using diethyl ether. The insoluble fraction, containing catalyst and insoluble polymer, was separated from the soluble fraction via centrifugation. The insoluble fraction was dried for 1 hour at 80 °C and weighed for the conversion calculation using Eq. (3).

$$\text{Conversion} = \left(1 - \frac{\text{Mass of insoluble fraction} - \text{Mass of catalyst}}{\text{Mass of initial polymer}}\right) \times 100\% \quad (3)$$

The soluble products were separated into aniline and polyol fractions using flash column chromatography with pentane/ethyl acetate (1:1) as the eluent, with a gradual increase of polarity by increasing the amount of ethyl acetate gradually up to pentane/ethyl acetate (1:4). Lastly, methanol was used to extract the polyol fraction. The solvent was removed on a rotary-evaporator, and the products were weighed and analysed by ^{1}H NMR spectroscopy in d_6-chloroform.

Data availability

The experimental data generated in this study have been deposited in the Zenodo database. https://doi.org/10.5281/zenodo.14762014.

References

1. Geyer, R., Jambeck, J. R. & Law, K. L. Production, use, and fate of all plastics ever made. *Sci. Adv.* **3**, e1700782 (2017).
2. Delebecq, E., Pascault, J.-P., Boutevin, B. & Ganachaud, F. On the Versatility of Urethane/Urea Bonds: Reversibility, Blocked Isocyanate, and Non-isocyanate Polyurethane. *Chem. Rev.* **113**, 80–118 (2013).
3. Randall, D. & Lee, S. *The Polyurethanes Book*. (Wiley, 2002).
4. Choffat, F., Corsaro, A., Di Fratta, C. & Kelch, S. 3 - Advances in polyurethane structural adhesives. in *Advances in Structural Adhesive Bonding (Second Edition)* (Woodhead Publishing, 2023).
5. Braun, H. Methylene Diphenyl Diisocyanate (MDI) and Toluene Diisocyanate (TDI). in *Industrial Arene Chemistry* 1525–1574 (Wiley, 2023).
6. Martín, A. J., Mondelli, C., Jaydev, S. D. & Pérez-Ramírez, J. Catalytic processing of plastic waste on the rise. *Chem* **7**, 1487–1533 (2021).
7. Adetunji, C. O., Olaniyan, O. T., Anani, O. A., Inobeme, A. & Mathew, J. T. Environmental Impact of Polyurethane Chemistry. in *Polyurethane Chemistry: Renewable Polyols and Isocyanates* vol. 1380 393–411 (American Chemical Society, 2021).
8. Mahoney, L. R., Weiner, S. A. & Ferris, F. C. Hydrolysis of polyurethane foam waste. *Environ. Sci. & Technol.* **8**, 135–139 (1974).
9. Johansen, M. B., Donslund, B. S., Henriksen, M. L., Kristensen, S. K. & Skrydstrup, T. Selective chemical disassembly of elastane fibres and polyurethane coatings in textiles. *Green Chem* **25**, 10622–10629 (2023).
10. Grdadolnik, M. et al. Chemical Recycling of Flexible Polyurethane Foams by Aminolysis to Recover High-Quality Polyols. *ACS Sustainable Chem. Eng.* **11**, 10864–10873 (2023).
11. Zahedifar, P., Pazdur, L., Vande Velde, C. M. L. & Billen, P. Multistage Chemical Recycling of Polyurethanes and Dicarbamates: A Glycolysis–Hydrolysis Demonstration. *Sustainability* **13**, 3583 (2021).
12. Simón, D., Borreguero, A. M., de Lucas, A. & Rodríguez, J. F. Recycling of polyurethanes from laboratory to industry, a journey towards the sustainability. *Waste Manage* **76**, 147–171 (2018).
13. Gausas, L. et al. Catalytic Hydrogenation of Polyurethanes to Base Chemicals: From Model Systems to Commercial and End-of-Life Polyurethane Materials. *JACS Au* **1**, 517–524 (2021).
14. Rong, H. et al. Theoretical Study on the Hydrogenolysis of Polyurethanes to Improve the Catalytic Activities. *Inorg. Chem.* **61**, 14662–14672 (2022).
15. Zhou, W. et al. Depolymerization of Technical-Grade Polyamide 66 and Polyurethane Materials through Hydrogenation. *ChemSusChem* **14**, 4176–4180 (2021).
16. Gausas, L., Donslund, B. S., Kristensen, S. K. & Skrydstrup, T. Evaluation of Manganese Catalysts for the Hydrogenative Deconstruction of Commercial and End-of-Life Polyurethane Samples. *ChemSusChem* **15**, e202101705 (2022).
17. Védrine, J. C. Heterogeneous Catalysis on Metal Oxides. *Catalysts* **7**, (2017).
18. Li, Z. & Huang, W. Reactivity of hydrogen species on oxide surfaces. *Sci. China Chem.* **64**, 1076–1087 (2021).
19. Aireddy, D. R. & Ding, K. Heterolytic Dissociation of H_2 in Heterogeneous Catalysis. *ACS Catal* **12**, 4707–4723 (2022).
20. Copéret, C., Estes, D. P., Larmier, K. & Searles, K. Isolated Surface Hydrides: Formation, Structure, and Reactivity. *Chem. Rev.* **116**, 8463–8505 (2016).
21. Taguchi, M., Ishikawa, Y., Kataoka, S., Naka, T. & Funazukuri, T. CeO_2 nanocatalysts for the chemical recycling of polycarbonate. *Catal. Commun.* **84**, 93–97 (2016).
22. García-Melchor, M. & López, N. Homolytic Products from Heterolytic Paths in H_2 Dissociation on Metal Oxides: The Example of CeO_2. *J. Phys. Chem. C* **118**, 10921–10926 (2014).
23. Kordomenos, P. & Kresta, J. Thermal stability of isocyanate-based polymers. 1. Kinetics of the thermal dissociation of urethane, oxazolidone, and isocyanurate groups. *Macromolecules* **14**, 1434–1437 (1981).
24. Tamura, M. & Tomishige, K. Redox Properties of CeO_2 at Low Temperature: The Direct Synthesis of Imines from Alcohol and Amine. *Angew. Chem. Int. Ed.* **54**, 864–867 (2015).
25. Yang, H., Garcia, H. & Hu, C. Hydrogenation of amides to amines by heterogeneous catalysis: a review. *Green Chem* **26**, 2341–2364 (2024).

26. Tomishige, K., Tamura, M. & Nakagawa, Y. CO_2 Conversion with Alcohols and Amines into Carbonates, Ureas, and Carbamates over CeO_2 Catalyst in the Presence and Absence of 2-Cyanopyridine. *Chem. Rec.* **19**, 1354–1379 (2019).
27. Beste, A. & Overbury, S. H. Pathways for Ethanol Dehydrogenation and Dehydration Catalyzed by Ceria (111) and (100) Surfaces. *J. Phys. Chem. C* **119**, 2447–2455 (2015).
28. Salcedo, A., Poggio-Fraccari, E., Mariño, F. & Irigoyen, B. Tuning the selectivity of cerium oxide for ethanol dehydration to ethylene. *Appl. Surf. Sci.* **599**, 153963 (2022).
29. Li, M., Wu, Z. & Overbury, S. H. Surface structure dependence of selective oxidation of ethanol on faceted CeO_2 nanocrystals. *J. Catal.* **306**, 164–176 (2013).
30. Wang, Y. et al. Complete CO Oxidation by O_2 and H_2O over Pt–CeO_2–δ/MgO Following Langmuir–Hinshelwood and Mars–van Krevelen Mechanisms. *Respectively. ACS Catal.* **11**, 11820–11830 (2021).
31. Xing, F., Nakaya, Y., Yasumura, S., Shimizu, K. & Furukawa, S. Ternary platinum–cobalt–indium nanoalloy on ceria as a highly efficient catalyst for the oxidative dehydrogenation of propane using CO_2. *Nat. Catal.* **5**, 55–65 (2022).
32. Lei, L., Wang, Y., Zhang, Z., An, J. & Wang, F. Transformations of Biomass, Its Derivatives, and Downstream Chemicals over Ceria Catalysts. *ACS Catal* **10**, 8788–8814 (2020).
33. Wu, X. et al. Controlling the selectivity of the hydrogenolysis of polyamides catalysed by ceria-supported metal nanoparticles. *Nat. Commun.* **14**, 6524 (2023).
34. O'Dea, R. M. et al. Toward Circular Recycling of Polyurethanes: Depolymerization and Recovery of Isocyanates. *JACS Au* **4**, 1471–1479 (2024).
35. Hinuma, Y. et al. Density Functional Theory Calculations of Oxygen Vacancy Formation and Subsequent Molecular Adsorption on Oxide Surfaces. *J. Phys. Chem. C* **122**, 29435–29444 (2018).
36. Mullins, D. R. The surface chemistry of cerium oxide. *Surf. Sci. Rep.* **70**, 42–85 (2015).
37. Mullins, D. R., Senanayake, S. D. & Chen, T.-L. Adsorption and Reaction of C_1–C_3 Alcohols over CeO_X(111) Thin Films. *J. Phys. Chem. C* **114**, 17112–17119 (2010).
38. Chen, T.-L. & Mullins, D. R. Ethylene Glycol Adsorption and Reaction over CeO_X(111) Thin Films. *J. Phys. Chem. C* **115**, 13725–13733 (2011).
39. Li, Z. et al. Interaction of Hydrogen with Ceria: Hydroxylation, Reduction, and Hydride Formation on the Surface and in the Bulk. *Chem. Eur. J.* **27**, 5268–5276 (2021).
40. Vilé, G., Bridier, B., Wichert, J. & Pérez-Ramírez, J. Ceria in Hydrogenation Catalysis: High Selectivity in the Conversion of Alkynes to Olefins. *Angew. Chem. Int. Ed.* **51**, 8620–8623 (2012).
41. Bhasker-Ranganath, S. & Xu, Y. Hydrolysis of Acetamide on Low-Index CeO_2 Surfaces: Ceria as a Deamidation and General De-esterification Catalyst. *ACS Catal* **12**, 10222–10234 (2022).
42. Kamachi, T. et al. Combined theoretical and experimental study on alcoholysis of amides on CeO_2 surface: A catalytic interplay between Lewis acid and base sites. *Catal. Today* **303**, 256–262 (2018).
43. Rass-Hansen, J., Falsig, H., Jørgensen, B. & Christensen, C. H. Bioethanol: fuel or feedstock? *J. Chem. Technol. Biotechnol.* **82**, 329–333 (2007).
44. Mudiyanselage, K., Al-Shankiti, I., Foulis, A., Llorca, J. & Idriss, H. Reactions of ethanol over CeO_2 and Ru/CeO_2 catalysts. *Appl. Catal. B Environ.* **197**, 198–205 (2016).
45. Yee, A., Morrison, S. J. & Idriss, H. A Study of the Reactions of Ethanol on CeO_2 and Pd/CeO_2 by Steady State Reactions, Temperature Programmed Desorption, and In Situ FT-IR. *J. Catal.* **186**, 279–295 (1999).
46. Ko, A.-N., Yang, C.-L., Zhu, W. & Lin, H. Selective N-alkylation of aniline with methanol over γ-alumina. *Appl. Catal. A Gen.* **134**, 53–66 (1996).
47. Datta, J. & Kasprzyk, P. Thermoplastic polyurethanes derived from petrochemical or renewable resources: A comprehensive review. *Polym. Eng. Sci.* **58**, E14–E35 (2018).
48. Desai, S. M., Sonawane, R. Y. & More, A. P. Thermoplastic polyurethane for three-dimensional printing applications: A review. *Polym. Adv. Technol.* **34**, 2061–2082 (2023).
49. Robert L. Strickman, Melvyn B. Strickman. *Polyurethane sponges manufactured with additive dispersed therein. Patent US 4271272A (1978)*
50. Hahladakis, J. N., Velis, C. A., Weber, R., Iacovidou, E. & Purnell, P. An overview of chemical additives present in plastics: Migration, release, fate and environmental impact during their use, disposal and recycling. *J. Hazard. Mater.* **344**, 179–199 (2018).
51. Vogt, B. D., Stokes, K. K. & Kumar, S. K. Why is Recycling of Post-consumer Plastics so Challenging? *ACS Appl. Polym. Mater.* **3**, 4325–4346 (2021).
52. Jiao, L., Xiao, H., Wang, Q. & Sun, J. Thermal degradation characteristics of rigid polyurethane foam and the volatile products analysis with TG-FTIR-MS. *Polym. Degrad. Stab.* **98**, 2687–2696 (2013).
53. Musa, A., Jaseer, E. A., Barman, S. & Garcia, N. Review on Catalytic Depolymerization of Polyolefin Waste by Hydrogenolysis: State-of-the-Art and Outlook. *Energy Fuels* **38**, 1676–1691 (2024).
54. Trovarelli, A., de Leitenburg, C., Boaro, M. & Dolcetti, G. The utilization of ceria in industrial catalysis. *Catal. Today* **50**, 353–367 (1999).

Acknowledgements

This publication was supported by the EPFL (Switzerland) and NCCR catalysis (grant number 180544), a National Centre of Competence in Research funded by the Swiss National Science Foundation (SNSF). N. Yan. thanks MOE Tier-2 project (MOE-T2EP10221-0020) from Ministry of Education, Singapore for financial support. The authors thank Daniel Ortiz, Francisco Sepulveda, Natalia Gasilova and Yann Lavanchy for their technical support.

Author contributions

X.W., R.C.T.-R. and P.J.D. contributed to the design of the experiments and data analysis. X.W. and J.C.S. performed the experiments, P.H. performed the NH_3-TPD and BET measurements and L.P. performed the ^{31}P MAS NMR measurements; X.W., N.Y. and P.J.D. wrote the manuscript and all authors discussed, commented on and proofread the manuscript.

Competing interests

The catalytic method is described in a patent invented by X.W. and P.J.D. (EP Patent, No. 24222874.0). The remaining authors declare no competing interests.

Additional information

Supplementary information The online version contains supplementary material available at https://doi.org/10.1038/s41467-025-59688-0.

Correspondence and requests for materials should be addressed to Ning Yan or Paul J. Dyson.

Peer review information *Nature Communications* thanks Fan Zhang and the other, anonymous, reviewer(s) for their contribution to the peer review of this work. A peer review file is available.